Rapid determination of the high cycle fatigue properties of high temperature aeronautical alloys by self-heating measurements

Vincent Roué[1,2,*], *Cédric* Doudard[1], *Sylvain* Calloch[1], *Frédéric* Montel[1], *Quentin* Pujol D'Andrebo[2] and *Fabien* Corpace[2]

[1]Institut de Recherche Dupuy de Lôme (IRDL) UMR 6027, ENSTA Bretagne, 29200 Brest, France
[2]Safran Aircraft Engines, Villaroche, 77550 Moissy-Cramayel, France

Abstract. The determination of high cycle fatigue (HCF) properties of a material with standard method requires a lot of specimens, and could be really time consuming. The self-heating method has been developed in order to predict S–N–P curves (*i.e.*, amplitude stress – number of cycles to failure – probability of failure) with only a few specimens. So the time-saving advantage of this method has been demonstrated on several materials, at room temperature. In order to reduce the cost and time of fatigue characterization at high temperature, the self-heating method is adapted to characterize HCF properties of a titanium alloy, the Ti-6Al-4V (TA6V), at different temperatures. So the self-heating procedure is adjusted to conduct tests with a furnace. Two dissipative phenomena can be observed on self-heating curves. Because of this, a two-scale probabilistic model with two dissipative mechanisms is used to describe them. The first one is observed for low amplitudes of cyclic loading, under the fatigue limit, and the second one for higher amplitudes where the mechanisms of fatigue damage are activated and are dissipating more energy. This model was developed on steel at room temperature. Even so, it is used to describe the self-heating curves of the TA6V at several temperatures.

1 Introduction

Performance of turbojet can be improved by increasing the operation temperature or by reducing the mass of the components. Consequently, jet engine parts are subjected to increasing stress load in environments in which the temperature increases. In the context of aircraft parts, HCF (high cycle fatigue) design method must be as accurate as possible and so a lot of fatigue tests are needed to study the influence of some parameters (temperature, mean stress,..) on the HCF properties of materials.

The material tested in this study is a titanium alloy the TA6V (Ti-6Al-4), widely used in aircraft industry. This material is often used for the construction of jet engine compressors. The pressure and also the temperature rise in the direction of the flow passing through the compressor, so multiple conditions of loads and temperatures must be studied to correctly design in fatigue the different parts of the compressor. Indeed, stator vanes and discs are subjected to vibratory loadings, so to a load ratio of around R=-1. Rotor blades are subjected to a high mean stress due to centrifugal forces in addition to the vibratory loadings, meaning the load ratio increases to around R=0.5 or R=0.7 depending on the case. Thus, the fatigue properties at several load ratios (the ratio between the minimal and the maximal cyclic stress applied on the specimen) and at different temperatures are needed for the TA6V.

However the determination method of the fatigue limit, arbitrarily set at the stress amplitude for a lifetime of 10^7 cycles, with the Staircase method requires a lot of specimens and time. Even more specimens are needed to correctly evaluate the dispersion of the fatigue properties. So this process is quite long and expensive, just to determine the HCF properties (limit and dispersion) for a given load ratio and temperature. So the purpose of this study is to develop a fast prediction method of HCF properties at high temperature (up to 450°C for the TA6V) based on self-heating measurements under cyclic loadings.

This method is based on the monitoring of the stabilized temperature of the studied specimen during cyclic loadings. Several consecutive blocks of a few thousand cycles with increasing stress amplitude are applied on the specimen. For each block (i.e. for each stress amplitude), the stabilized temperature of the specimen is determined. An empirical interpretation of this evolution allows the obtaining of an estimation of the endurance limit [1,2]. Indeed, the fatigue mechanisms are also dissipative mechanisms. So when the stress amplitude applied on the specimen is higher than the endurance limit, theses mechanisms are dissipating energy and the temperature of the specimen rises, which allows us to estimate the endurance limit of the material.

The self-heating method, or a similar method, has been used on different materials : a wide range of steel [3,4], composite materials [5] and elastomeric materials

* Corresponding author: vincent.roue@safrangroup.com

[6]. It has also been used for different load ratios [7] and extended to multiaxial loadings [8,9]. In all of these cases, the link between self-heating measurements and fatigue properties (at least the mean endurance limit) is established. Self-heating methods could also be used to quickly quantify the influence of various parameters (such as mean stress effect [7] or plastic prestrain [3]) on fatigue properties.

In this paper, we propose an extension of the use of self-heating measurement to the prediction of HCF properties of the TA6V at different temperatures (up to 450°C). Moreover, different load ratios are studied to demonstrate the capability of the HCF properties predictions with the self-heating method. The purpose is to quickly obtain a Goodman-Haigh diagram for endurance limits at the different temperature used during the fatigue design of the components. This study seeks to reduce the time and cost of the characterization of fatigue properties characterization of materials, in order to fulfil industrial needs.

Moreover, this method allows the study of fatigue mechanisms without creep influence. Indeed, during classical fatigue tests at high temperature, specimen rupture could be due to creep damage because of low frequencies used during fatigue testing (around 100Hz), while actual parts are subjected to high frequencies (around 20kHz). So the parts are less subjected to creep damage than the specimens used to determine fatigue properties. However, during self-heating measurements, only a few thousand cycles are applied on the specimen, which is enough to reach the stabilization of the measured temperature. So, the endurance limit could be determined with this method without creep influence.

This paper is divided into three parts. The first part describes the development and performance of self-heating tests at high temperature. It presents the adjustments made to the procedure to conduct tests with a furnace. The self-heating results are also presented for several conditions of temperature and load ratio. The second part presents the two-scale probabilistic model with the two dissipative phenomena developed by Munier et al. [3], and used here as a first approach to analyze the self-heating curves. This section describes the principle of the model and presents the calculation of the dissipation. Thus, the heat conduction equation can be solved and the experimental self-heating measurements can be described. The link with the HCF properties is also presented. Finally, in the third section, the model is applied on the self-heating results to determine the HCF properties of the material. The empirical determination of the mean endurance limit (corresponding to a probability of failure of 50% at 10^7cycles) is presented. Finally, the results predicted by the model are compared to classical experimental fatigue results.

2 Self-heating test procedure at high temperature

The self-heating test procedure is well established to perform tests at room temperature on metal alloys [2,3]. The procedure is adapted here to conduct tests with a furnace and to be able to measure a low rise of the specimen temperature (the self-heating temperature) at high temperature (up to 450°C).

In this section, the specimen and the experimental device are presented. So adjustments to conduct self-heating measurement with the furnace are briefly explained. Then the procedure of the self-heating measurements under cyclic loadings is presented and applied to one example of temperature and load ratio (T=250°C and R=-1).

2.1 Experimental device

In order to be able to measure a low rise of the specimen temperature at high temperature, the procedure and the experimental device are adapted to improve and optimize the temperature signals. Some precautions are needed to reduce signals noise. Moreover the heating system and its regulation must be chosen to have the best environmental temperature, with small temperature variations and a good temperature stabilization. The regulation of the system must not be linked directly to the specimen temperature. Indeed, if it is the case, the self-heating of the specimen could disrupt the regulation of the environmental temperature.

The aim of this subsection is to propose an experimental protocol to study the effect of the temperature on the HCF properties. All the specimens are tested under the same conditions, with the same procedure and device.

2.1.1 Specimen and experimental set-up

The experimental set-up is composed of the hydraulic machine, the furnace split in three different zones allowing a better regulation of the temperature and high temperature reverse-stress pullrods with water-cooled collet grips (Figure 1).

The geometry of the specimen in the zone of interest is a cylindrical shape (Figure 2). The ends of the specimen are threaded and interface parts had been developed to enable cyclic loadings at high temperature. The specimen geometry had been developed by Safran and it is the geometry used during classical fatigue tests. All specimens were provided by Safran, and all underwent the same manufacturing process.

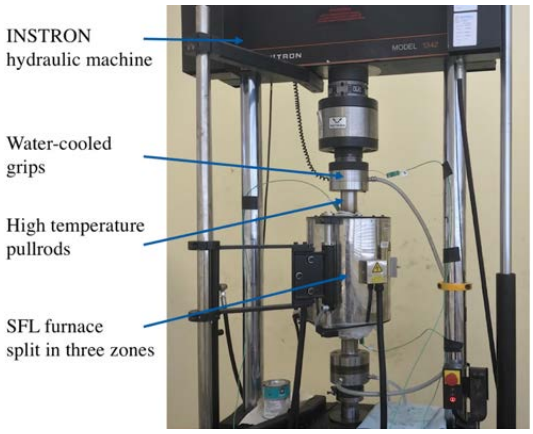

Fig. 1. Experimental device for the self-heating test at high temperature.

This heating technology and so this furnace were chosen because it enables the environment to maintain a stable temperature, with a certain inertia. The regulation of the furnace has a long characteristic time, which allows us to consider the environmental temperature during the self-heating procedure as constant. Indeed, the duration of one block of cyclic loading is shorter than the furnace characteristic time.

The pullrods must be cooled to protect the cell and the hydraulic system of the machine. So one of the main sources of thermal losses is through conduction in the pullrods. Other thermal losses, such as convective losses, are reduced as much as possible by controlling the thermal boundary conditions. So the thermal environment is as stable as possible to reduce the noise on thermal signals.

2.1.2 Temperature acquisition

A 0D approach is adopted in this paper (*i.e.* only the mean temperature elevation of the specimen is considered). Therefore, a thermocouple is sufficient to measure the mean temperature of the specimen in the region of interest. In the same way as the self-heating procedure at room temperature, three thermocouples are required, one is fixed on the center of the specimen and the other two are fixed on the high temperature grips (Figure 2). The thermocouples of the grips are close enough to the specimen to measure the variation of temperature in its immediate environment, without measuring the rise of temperature during its self-heating.

To reduce the thermal noise as much as possible and reduce the variations of the environmental temperature, we must control the thermal boundary conditions. The most important issue is to avoid stack effect, which greatly deteriorates the thermal signal, hence the precautions taken to block the air flow (rock wool, ceramic fiber cord, etc.).

The relative accuracy of the measuring system, from the type K thermocouples used and through the electronic conditioner, is lower than 0.01 K. Its response time is of the order of one second, so the acquisition frequency is set at 1 Hz. Thus, the temperature elevation of the specimen θ is given by

$$\theta = T_S - \frac{T_{UG} + T_{LG}}{2}, \quad (1)$$

with T_S the temperature in the region of interest of the specimen, T_{UG} the temperature of the uppergrip and T_{LG} the temperature of the lowergrip. Unlike the procedure at room temperature, an offset is often needed to correct the elevation of temperature of the specimen θ. Indeed, the temperatures of the grips are lower than the temperature in the center of the specimen as a result of the water-cooled system and the conduction losses through the pullrods (Figure 4). The θ temperature is rapidly stabilized and reaches a constant temperature. It allows us to predict the temperature drift and perform self-heating measurements even before the complete stabilization of the temperature in the furnace. The self-heating temperature is the temperature θ more or less the offset of the stabilized value of θ.

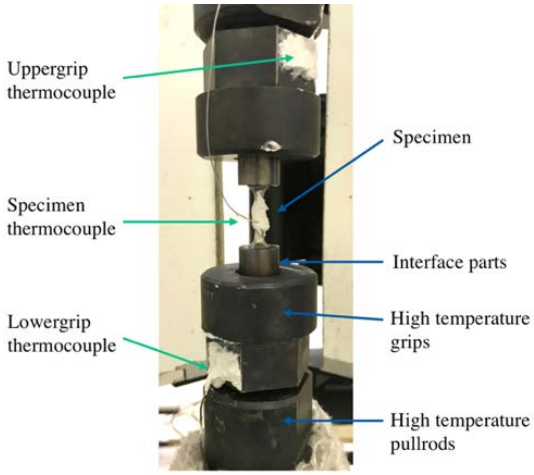

Fig. 2. Geometry of the specimen and thermocouples fixing.

Moreover, the specimen is quite small in comparison with the pullrods and the furnace, and so the self-heating of the specimen does not disrupt the environmental temperature. It allows us to measure the self-heating of the specimen ranging from small rises in the specimen temperature (around 0.04 K), with the optimization of the temperature signals due to the precautions taken for temperature acquisition and noise reduction of the environmental temperature, to quite important rises of the specimen temperature (around 10 K), without any interference in the furnace regulation.

So after stabilization of the θ temperature, the relative resolution is still lower than 0.01 K. The thermal noise of the measuring system is around 0.03 K. The stabilized temperature is still oscillating due to the regulation of the furnace, external perturbations and losses. The amplitude of the oscillations is around 0.1 K, but its frequency is sufficiently low to be predictable and perform a block of cycling loadings during a self-heating procedure.

2.2 Self-heating procedure

Given that the measuring system is set up and optimized to seek small elevation of temperature at high

temperature, self-heating measurements of the specimen can now be done at high temperature.

So in this subsection, the self-heating method under cyclic loadings is presented. The procedure is applied to one condition of temperature and load ratio (T=250°C and R=-1) as an example.

2.2.1 Loading conditions

A complete self-heating test consists of the application of a successive series of cyclic loadings, with increasing stress amplitude Σ_0 (Figure 3). All the blocks of cyclic loading are performed at the same frequency, 30 Hz, and with the same number of cycles, 6000 cycles. Moreover, they are performed at the same load ratio R (depending of the chosen conditions for each specimen), given by

$$R = \frac{\sigma_{min}}{\sigma_{max}}, \quad (2)$$

with σ_{min} the minimum stress applied during the block of cycling loading and σ_{max} the maximum stress. For the example, the load ratio is fixed at R=-1, so $\sigma_{min} = -\Sigma_{0_i}$ and $\sigma_{max} = \Sigma_{0_i}$.

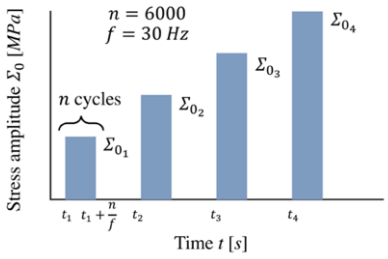

Fig. 3. Successive series of cyclic loadings with increasing stress amplitudes.

2.2.2 Self-heating temperature

During each cyclic loading block, the temperature elevation θ is registered. Few examples of thermal responses are presented on Figure 4. The stress $\Sigma_{\max}$ is used to normalize all the stresses represented in this paper. The value was set arbitrarily.

Figure 4 shows the evolution of temperature elevation for few loading steps. During each of them, a "steady-state" temperature $\bar{\theta}$ is determined. In fact, the temperature elevation does not reach a stabilized value for every loading step. More cycles should have been done to possibly reach a steady-state temperature. Actually, some longer cyclic loadings had been done, and the elevation of temperature does not seem to stabilize. Anyway, the "steady-state" temperature $\bar{\theta}$ is evaluated during the same period of time at the end of each loading step, given that the thermal conditions are the same. Indeed the characteristic time to reach thermal balance (evaluated during the cooling of the specimen) is the same for every loading step. Few errors could be made with this analysis, but we can still study the evolution of this steady-state temperature $\bar{\theta}$ as a function of the stress amplitude Σ_0 applied during the cyclic loading. Indeed, any errors would be constant in each loading step, and we are only interested by the evolution of this steady-state temperature $\bar{\theta}$. Thus, Figure 4 shows that the steady-state temperature $\bar{\theta}$ increases with the stress amplitude Σ_0.

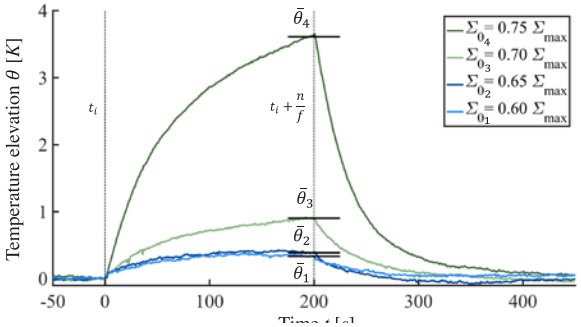

Fig. 4. Evolution of the mean temperature elevation during several blocks of cyclic loadings.

2.2.3 Self-heating curve

At the end of the self-heating test, a self-heating curve is obtained. It represents the steady-state temperature $\bar{\theta}$ relating to the stress amplitude Σ_0 (Figure 5). The self-heating curve is also plotted in a logarithmic scale to clarify the presence of the two self-heating regimes : the first for low amplitudes is called the primary regime and the second one for highest amplitudes [3,4].

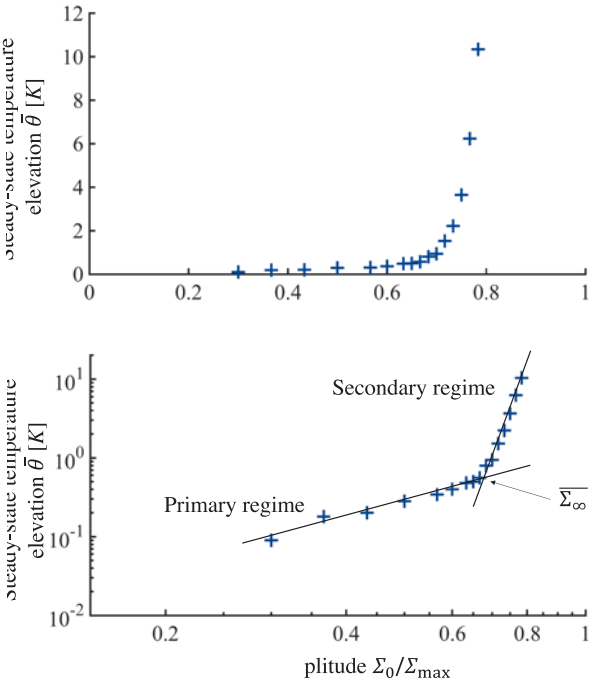

Fig. 5. Self-heating curve for the condition T=250°C and R=-1.

The primary regime has a slope of two in the logarithmic diagram, in accordance with the observations of Munier on steels at room temperature [3,4]. The secondary regime has a higher slope in the logarithmic diagram. This regime is associated with the progressive appearance of microplasticity [2]. Indeed, this regime is associated with the appearance of fatigue

damage. In the model, it is used to determined fatigue properties of the material.

The empirical determination of the mean endurance limit proposed by Munier concerned an endurance limit set at the order of 10^6 cycles. For aeronautical applications, the endurance limit is defined for a number of cycles of 10^7. Thus, the empirical determination of the mean endurance limit exposed in this paper is slightly different. This limit $\overline{\Sigma_\infty}$ is determined as the amplitude for which the secondary regime appears (Figure 5).

2.3 Self-heating results at several temperatures

In this subsection, the self-heating curves obtained for several conditions of temperatures and loading ratios are presented. The curves are briefly described, and the main observations made during the tests are noted.

2.3.1 Load ratio effect on self-heating curves

Figure 6 shows the effect of the load ratio on self-heating curves. Three load ratios are presented, R=-1, R=0 and R=0.5 for the temperature T=250°C.

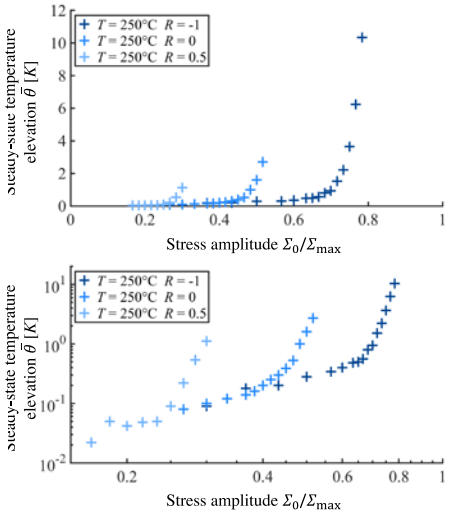

Fig. 6. Influence of the loading ratio R on the self-heating curves for the temperature T=250°C.

The self-heating curves obtained at different load ratios seem to have the same primary regime. Moreover, the secondary regime is activated at lower stress amplitude when the load ratio increases. This regime is correlates with the fatigue damage, meaning the fatigue properties of the TA6V decrease when the load ratio increases. Indeed, when the load ratio is R=0 or R=0.5, a mean stress is applied and the maximum stress is higher ; so the endurance limit is lower.

2.3.2 Temperature effect on self-heating curves

Figure 7 shows the evolution of self-heating curves with the temperature. Two temperatures (250°C and 450°C) were tested at a load ratio of R=0.

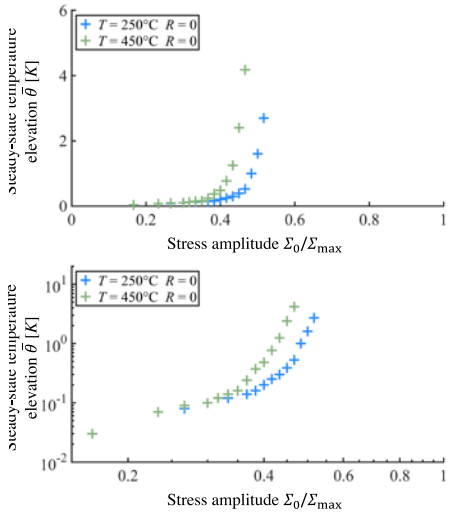

Fig. 7. Influence of the temperature on the self-heating curves for the loading ratio R=0.

The secondary regime is activated at lower stress amplitude when the temperature increases, so the fatigue properties decrease when the temperature is higher.

All the self-heating curves presented in this paper seem to have the same primary regime. It also has a slope value of two in the logarithmic diagram, in accordance with Munier's observations on steel at room temperature [4].

However, the beginning and the intensity of the secondary regime depend on the conditions of testing. The self-heating curves show that the secondary regime is activated at lower stress amplitude when the load ratio or the temperature increase. Indeed, the fatigue properties are affected with the presence of a higher mean stress or a higher environmental temperature.

3 The two-scale probabilistic model with dissipative mechanisms

The aim of this section is to present and summarize the two-scale probabilistic model developed by Munier et al. [3] on a wide range of steels at room temperature. Indeed, the presence of two regimes on the self-heating curves of the TA6V and other experimental observations (influence of the frequency, etc.) impel us to use this model as a first approach, although the dissipation mechanisms for the TA6V are not yet clearly determined.

Firstly, the principle of the model is displayed. Then the dissipated energy calculation is presented. It enables us to solve the heat conduction equation and describe the self-heating curves. Finally, the link with fatigue properties is presented.

3.1. Principle of the model and Representative Elementary Volume

The description of the two regimes requires the presence of two dissipative mechanisms. So the Representative Elementary Volume (REV) is defined as an elasto-plastic matrix containing a set of inclusions [3,4]. The

set of inclusions represent microplasticity sites, with an additional plastic hardening. So under low amplitude cyclic loadings, the inclusions have the same behavior as the matrix, and so its dissipation is the same. Above a given stress amplitude threshold (different for each inclusion), the inclusion is activated and another dissipation appears. This stress amplitude threshold is defined as a probabilistic variable, and it represents the population of inclusions in the REV. So the dissipation associated with the matrix corresponds to the primary regime. The secondary regime is then associated to the dissipation of the inclusions. The REV is represented in Figure 8.

The sites activation represents the process of fatigue damage initiation. Thus, the analysis of the secondary regime allows us to determine fatigue properties of the material.

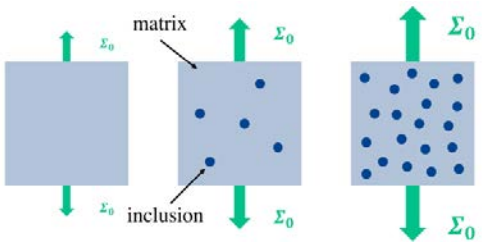

Fig. 8. Principle and REV of the two-scale probabilistic model.

3.2. Thermodynamic framework and dissipated energy calculation

In this subsection, the matrix behavior and the behavior of one inclusion are presented. Then the activation scenario of the sites, and so the behavior of the set of inclusions, is presented.

3.2.1 Dissipation in the matrix

The dissipation of the matrix is associated with the primary regime, which has a slope of two in a logarithmic diagram. So Munier et al. [3,4] proposed a framework for which the mean steady-state temperature $\bar{\theta}$ is a quadratic function of stress amplitude Σ_0. This result is obtained by defining a non-linear kinematic hardening for the matrix and by introducing a specific pseudo-potential.

So the dissipation can be calculated for one cycle of loading. Then the cyclic dissipative energy density (integration of the intrinsic dissipation over one cycle) can be approximated by a quadratic function of the stress amplitude

$$E_d^{mat} \approx K\,\Sigma_0^2, \tag{3}$$

with K depending on several model parameters.

3.2.2 Dissipation in one inclusion under cyclic loading

One inclusion is defined by its stress amplitude threshold σ_y^μ. If the stress applied within the inclusion (which is not the same as the macro-stress amplitude Σ_0) is lower than this threshold, the behavior of the inclusion is the same as the matrix. In this part, let us assume that the stress applied within the inclusion is greater than that of the threshold. An additional hardening is activated, and the dissipation of the inclusion is no longer the same as the matrix.

A localization law is needed to describe the relation between the stress applied on the inclusion and the macro-stresses applied on the REV. This relation is deduced from Eshelby analysis [10]. The activated hardening of the inclusion is defined by a linear kinematic hardening [2,3]. Then the cyclic dissipative energy density can be calculated. Indeed, during a tension-compression cyclic loading and if $\Sigma_0 > \sigma_y^\mu$, it can be written as

$$E_d^{inc}(\sigma_y^\mu) \approx \frac{4\,\sigma_y^\mu}{h^\mu}\,\langle \Sigma_0 - \sigma_y^\mu \rangle, \tag{4}$$

with h^μ depending on the hardening parameters and the localization law parameters.

3.2.3 Activation of the population of inclusions and dissipation in the REV

The activation threshold σ_y^μ is a probabilistic variable. It is assumed to be described by a Point Poisson Process, so no spatial correlations are considered. Thus the number of active sites in a domain Ω of volume V is given by

$$N(\Omega) = \lambda V, \tag{5}$$

with λ the mean density of active sites in the volume. It is also assumed that λ follows a power law of the stress amplitude, given by [2]

$$\lambda = \frac{1}{V_0}\left(\frac{\Sigma_0}{S_0}\right)^m, \tag{6}$$

with m and $V_0 S_0^m$ two material parameters.

Experimental observations of persistent slip bands on some steel have shown that a power-law dependence could represent this appearance of sites [3]. Moreover, when this choice is made in addition to the weakest link assumption, the probability of failure is the same as the Weibull model [2].

So the cyclic dissipative energy density can be now calculated in the REV, it is given by

$$E_d = K\,\Sigma_0^2 + \int_0^{\Sigma_0} E_d^{inc}(\Sigma)\,\frac{V_s}{V}\,dN_a(\Sigma)\,d\Sigma, \tag{7}$$

with V_s the volume of one site and dN_a the number of sites activated between a stress amplitude of Σ and $\Sigma + \mathrm{d}\Sigma$. This number is obtained with the mean density of active sites λ,

$$dN_a(\Sigma) = V\left(\lambda(\Sigma + \mathrm{d}\Sigma) - \lambda(\Sigma)\right) = \mathrm{V}\frac{d\lambda}{d\Sigma}d\Sigma. \tag{8}$$

Thus the cyclic dissipative energy density is finally given by

$$E_d = K\,\Sigma_0^2 + \frac{4}{h^\mu}\,\frac{V_s}{V_0 S_0^m}\,\frac{\Sigma_0^{m+2}}{(m+1)(m+2)}. \tag{9}$$

3.3. Description of self-heating curves

In order to describe self-heating curves, the heat conduction equation must be solved. With the 0D approach, this equation is given by [4]

$$\dot{\theta} + \frac{\theta}{\tau_{eq}} = \frac{f}{\rho c} E_d, \quad (10)$$

with τ_{eq} the characteristic time of thermal equilibrium (depending on the testing conditions, specimen geometry, etc.), f the loading frequency, ρ the material density and c the specific heat. Therefore, the mean steady-state temperature elevation $\bar{\theta}$ can be written as a function of the stress amplitude Σ_0 and is given by

$$\bar{\theta} = \alpha \left(\frac{\Sigma_0}{\Sigma_{\max}}\right)^2 + \beta \left(\frac{\Sigma_0}{\Sigma_{\max}}\right)^{m+2}, \quad (11)$$

with α and β two constants defined from the previous parameters and results. This equation allows us to describe a self-heating curve, in accordance with the experimental observations, with three parameters :

- the intensity of the primary regime α, related to the cyclic dissipation of the matrix;
- the intensity of the secondary regime β, associated with the cyclic dissipation of the population of inclusions;
- the slope of the secondary regime m, related to the gradual appearance of active sites (from the definition of λ).

3.4. Prediction of fatigue properties

According to the model, it is assumed that the activation of the second kinematic hardening within the inclusion governs the process of fatigue damage initiation. So the evaluation of fatigue properties is done with the secondary regime of the self-heating curve. Thus the probability of finding k active sites in a domain Ω of volume V is given by [11]

$$P_k(V) = \frac{(\lambda k)^k}{k!} e^{-\lambda V}. \quad (12)$$

Moreover, the weakest link theory is assumed in the model. So the probability of failure P_F is equal to the probability of finding at least one active site,

$$P_F = P_{k\geq 1} = 1 - P_{k=0}. \quad (13)$$

By using the definition of λ, the probability of failure P_F is given by

$$P_F = 1 - \exp\left(-\frac{V}{V_0}\left(\frac{\Sigma_0}{S_0}\right)^m\right). \quad (14)$$

This equation corresponds to the Weibull model [12], with m representing the Weibull modulus. It is well known that this model takes into account the effect of volume on HCF properties. In order to take the stress heterogeneities effect into account, the concept of effective volume is introduced [13]. From the definition of the probability of failure, the mean endurance limit and the corresponding standard deviation are given by

$$\overline{\Sigma_\infty} = S_0 \left(\frac{V_0}{V_{eff}}\right)^{\frac{1}{m}} \Gamma\left(1 + \frac{1}{m}\right) \quad (15)$$

and

$$\overline{\overline{\Sigma_\infty}} = S_0 \left(\frac{V_0}{V_{eff}}\right)^{\frac{1}{m}} \sqrt{\Gamma\left(1 + \frac{2}{m}\right) - \Gamma^2\left(1 + \frac{1}{m}\right)}, \quad (16)$$

where Γ is the Euler gamma function and V_{eff} is the effective volume of the specimen. These last two equations show that the scatter of fatigue properties is only dependent of the Weibull modulus m, which can be directly identified on a self-heating curve. Indeed, it represents the slope of the secondary regime [2,3]. The energetic criterion used to describe S-N-P curves is not discussed in this paper.

4 Self-heating results and validation

In this last section, the two-scale probabilistic model is applied on the self-heating curves. Then the predictions are compared to some classical fatigue tests.

4.1. Identification of the model parameters

The primary regime is the same for all self-heating curves, so the intensity of the primary regime α is identify on all the curves and has an identical value for all of them.

The self-heating curves obtained with an applied mean stress (*i.e.* R=0 and R=0.5) could be altered by other dissipative mechanisms for high stress amplitude. The maximum stress for the last loading steps is often really close to the macroscopic elasticity limit, so the slope of the secondary regime is only identified for the self-heating curve obtained at R=-1. This allows us to identify the slope of the secondary regime m, which is also fixed for all the other curves. Indeed, it represents the set of inclusions in the specimens, which are all the same (Figure 9).

The only parameter left is β, the intensity of the secondary regime which depends on the testing conditions (T and R). This parameter is identified for all the curves to fit with the last points of the self-heating curves.

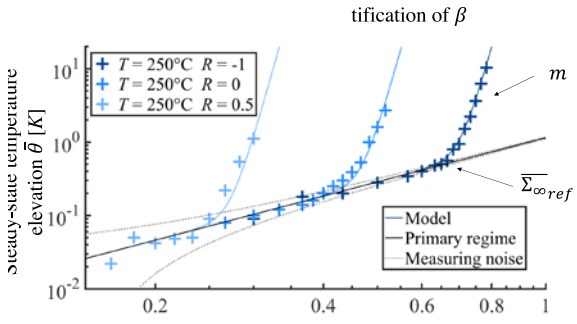

Fig. 9. Analysis of the self-heating curves and identification of the model parameters.

4.2. Empirical determination of the mean endurance limit

Indeed, it is possible to determine the mean fatigue limit with the parameter β with the equation

$$\overline{\Sigma_\infty} = \overline{\Sigma_\infty}_{ref} \left(\frac{\beta_{ref}}{\beta}\right)^{\frac{1}{m}}. \quad (17)$$

Thus, a couple of values $(\beta_{ref}, \overline{\Sigma_\infty}_{ref})$ are needed to determine the fatigue properties for all conditions of temperature and load ratio.

These two values are determined by the identification of the parameter β_{ref} on a self-heating curve and with an empirical determination of its mean endurance limit $\overline{\Sigma_\infty}_{ref}$. The chosen reference self-heating curve is the curve for the condition R=-1 (for the same reasons as previously) and T=250°C. Figure 9 shows the empirical determination of $\overline{\Sigma_\infty}_{ref}$ as the stress amplitude for which the secondary regime begun.

This method allows us to determine the mean endurance limit for each presented condition in this paper. It is possible to represent these results in a Haig diagram (Figure 10). Each point represents one specimen and was obtained in only one day.

4.3. Comparison with classical fatigue tests

The comparison with classical fatigue tests must still be done to validate the method. Figure 11 shows the comparison with some fatigue tests from Safran database. These fatigue tests were performed on specimens with identical geometry, but obtained from a different process.

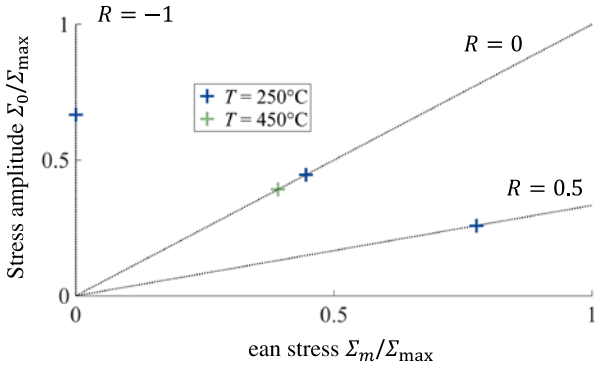

Fig. 10. Haig diagram obtained by self-heating measurements.

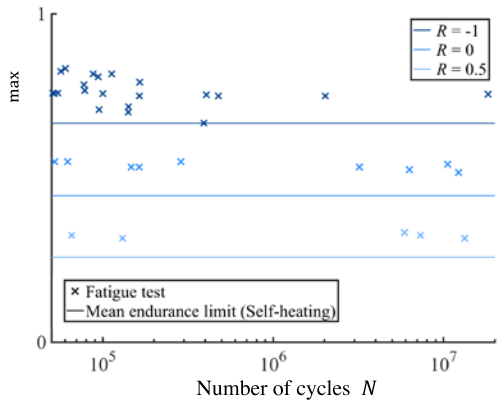

Fig. 11. Comparison of mean endurance limits obtained by the self-heating method with classical fatigue tests at 250°C.

Complementary fatigue tests must be performed to properly compare these self-heating results. However, there is a clear trend and the self-heating method at high temperature looks promising in reducing the time and cost of fatigue characterization at high temperature.

The scatter of the fatigue limit must also be analysed through classical fatigue tests to compare with the slope of the secondary regime and the parameter m.

5 Conclusion and perspectives

The present paper was devoted to the extension of the use of self-heating method under cyclic loadings for the prediction of HCF at different temperatures (up to 450°C). The purpose is to quickly obtain a Goodman-Haigh diagram for endurance limits at different temperatures. This study seeks to reduce the time and cost of the characterization of fatigue properties of materials, to fulfill industrial requirements.

The self-heating procedure and temperature acquisition were adapted to measure small increases in temperature corresponding to the self-heating of the specimen at high temperature. This paper has presented some examples of self-heating curves for different combinations of temperature and load ratio. These curves demonstrates the influence of the loading ratio and the temperature; the HCF properties identified with the self-heating curves can be seen to decrease when the temperature increases and in the presence of a mean stress. Indeed, we are able to measure the self-heating of specimens at high temperature. Dissipative mechanisms are well activated. For the TA6V, complementary studies and observations must be done to clearly identify these mechanisms. However, the presence of two regimes on the self-heating curves impels us to use a two-scale probabilistic model, developed on steel at room temperature, as a first approach.

A new empirical method is proposed to determine the mean endurance limit, set at the stress amplitude of a 10^7cycles lifetime. Complementary fatigue tests must be performed to validate the self-heating results, but thus far, the results have been promising. Self-heating measurements under other conditions of temperatures and loading ratios will be tested on the TA6V to quickly obtain a Haigh diagram.

Moreover, some other aspects of the two-scale probabilistic model must be studied. For example, the link between the fatigue dispersion and the slope of the secondary regime. The application of an energetic criterion could also be used to describe S-N-P curves.

The self-heating method at high temperature is a promising possibility for reducing the time and cost of the characterization of HCF properties. The use of this method could also be interesting at greater temperature, for the fatigue design of turbine parts.

References

1. C. E. Stromeyer. Proc Roy Soc London, A **90**, 411-425 (1914)

2. C. Doudard, S. Calloch, F. Hild, P. Cugy, A. Galtier. Fatigue Fract Eng Mat struct, **3**, 279-288 (2005)
3. R. Munier, C. Doudard, S. Calloch, B. Weber. Int J Fatigue, **63**, 46-61 (2014)
4. R. Munier. PhD Thesis (2012)
5. L. Jegou, Y. Marco, V. Le Saux, S. Calloch. Int J Fatigue, **47**, 259-267 (2013)
6. V. Le Saux, Y. Marco, S. Calloch, C. Doudard, P. Charrier. Int J Fatigue, **32**, 1582-1590 (2010)
7. G. La Rosa, A. Risitano. Int J Fatigue, **22**, 65-73 (2000)
8. C. Doudard, M. Poncelet, S. Calloch, C. Boué, F. Hild, A. Galtier. Int J Fatigue, **29**, 748-757 (2007)
9. M. Poncelet, C. Doudard, S. Calloch, B. Weber,A. Galtier. J Mech Phys Solids, **58**, 578-593 (2010)
10. E. Kröner. Acta Met, **9**, 155-161 (1984)
11. R. Gulino, S. L. Phoenix. J Mater Sci, **11**, 3107-3118 (1991)
12. W. Weibull. J Appl Mech, **18**, 293-297 (1951)
13. F. Hild, R. Billardon, D. Marquis. C R Acad Sci Paris, II **315**, 1293-1298 (1992)